

How well do operational models represent drizzle and light rain when compared with radar and lidar observations?

EWAN J. O'CONNOR*, ANTHONY J. ILLINGWORTH, ROBIN J. HOGAN AND CHRISTOPHER D. WESTBROOK

Department of Meteorology, University of Reading, United Kingdom

Submitted to J. Climate 18 August 2006; Revised October 2007;

ABSTRACT

Both climate and operational forecast models have difficulty representing the drizzle process, which is crucial in simulating stratocumulus and predicting their persistence and break-up. In this paper we use eighteen months of ground-based radar, lidar and disdrometer observations to derive statistics of the liquid water flux (i.e. precipitation rate) at cloud-base and at the ground for four operational forecast models. Occasions when there is any precipitation flux at the freezing level are excluded from the analysis, and only clouds warmer than 0°C and less than 1.5 km deep are included. Although the PDFs of modeled and observed liquid water paths are broadly similar, the four models all produce light drizzle ($< 0.1 \text{ mm hr}^{-1}$) at cloud-base much too frequently, and too much of this light drizzle reaches the ground. This is especially true for the ECMWF and Météo France models where most rainrates down to 0.001 mm hr^{-1} at cloud-base survive the journey to the ground. The Met Office model assumes an exponential drop size spectrum for the precipitation so at these low rainrates the small drops evaporate before reaching the ground. However, for rain rates of 0.03 to 1 mm hr^{-1} the evaporation rate is still too low; we suggest that their assumed Marshall-Palmer size distribution leads to drizzle drops which are too large. Observations suggest that in drizzle the intercept parameter of an exponential distribution, N_0 , is not constant but varies with the median volume diameter, D_0 , as D_0^{-k} , where k is typically in the range $1.5 - 2$. We propose a more appropriate power law relationship between liquid water flux (LWF) in $\text{kg m}^{-2} \text{ s}^{-1}$ and D_0 in m: $\text{LWF} = 5.37 \times 10^3 D_0^{2.50}$, suitable for drizzle drops with diameters from $80 \mu\text{m}$ to 1 mm . This result is explained physically in terms of number flux density.

1. Introduction

Stratocumulus clouds cover a large fraction of the Earth's surface (Hartmann *et al.*, 1992) and have a strong influence on the radiation budget of the Earth and hence climate (Ramanathan *et al.*, 1989; Harrison *et al.*, 1990). Climate models display significant errors in the climatology of stratocumulus (Jakob, 1999; Webb *et al.*, 2001; Jakob, 2003).

The presence of drizzle can alter the numerous feedback mechanisms that are involved in the continual generation of stratocumulus such as the entrainment rate, heat fluxes and water budgets (e.g. Caldwell *et al.*, 2005; Wood and Bretherton, 2004). For instance, the evaporation of drizzle below cloud causes cooling which can lead to decoupling (Nicholls, 1984; Albrecht *et al.*, 1995). Drizzle drops interspersed within the cloud can change the cloud droplet spectra and alter the cloud optical properties (Feingold *et al.*, 1996, 1997). This has an impact on radiative fluxes (Hudson and Yum, 2001) and, in turn, processes in the boundary layer that generate stratocumulus, such as turbulence and vertical redistribution of heat and moisture (Driedonks and Duynkerke,

1989; Paluch and Lenschow, 1991; Feingold *et al.*, 1996).

All these processes occur on small scales and hence are difficult to parametrize in numerical models (Wood, 2005). Indeed, the same precipitation scheme is used to represent both drizzle or rain produced by collision and coalescence, and rain arising from melting ice, even though the size distributions may be markedly different. Since drizzle is present in a significant proportion of stratocumulus clouds (Stephens *et al.*, 2002; Fox and Illingworth, 1997; O'Connor, 2003), an accurate representation of the drizzle process in numerical models is of interest. The inclusion of this process in models is not straightforward though, because the patchy nature of drizzle (van Zanten *et al.*, 2005; Comstock *et al.*, 2004) means that the process is not explicitly resolved at typical current operational model resolutions and has to be parametrized. Since the relationship between cloud water and any precipitation is expected to be non-linear, large biases in the modeled drizzle rate can be introduced if derived using grid-box-mean values (Pincus and Klein, 2000). In the precipitation schemes of current operational models, a simple estimate of the subgrid-scale variability is made through the use of the cloud fraction variable, which describes the proportion of a grid box filled with cloud. The

*Corresponding author address: Ewan J. O'Connor, Department of Meteorology, The University of Reading, Earley Gate, PO Box 243, Reading RG6 6BB, United Kingdom.
E-mail: e.j.oconnor@reading.ac.uk.

grid-box-mean cloud liquid water content is redistributed to occupy the cloudy fraction of the grid-box and the liquid water flux is then calculated from this in-cloud value.

In this paper the representation of drizzle and light rain in four operational forecast models is evaluated. We use a combination of radar and lidar observations of liquid water flux and drop size (O'Connor *et al.*, 2005), cloud liquid water path from microwave radiometer and surface precipitation rates and drop size from disdrometer. In our analysis we consider only occasions when warm rain processes are operating and specifically exclude the influence of the ice phase or any times when there is vigorous convection. This is achieved by excluding all observations and model representations when there is any precipitation flux at the freezing level so that only warm clouds remain; vigorous convective clouds are excluded by considering only those clouds less than 1.5 km deep. Liquid water fluxes (precipitation rates) at cloud base and the ground can easily be extracted from the model analysis. We examine the liquid water flux just below cloud base to isolate the precipitation generation terms (accretion and autoconversion) from the evaporation term, which can be estimated by comparing cloud base fluxes with those at the ground. For the observations, cloud base is estimated to within 30 m using vertically pointing lidar, which is straightforward (apart from certain multi-layered situations), and the precipitation rate just below cloud base is derived from the 60 m resolution reflectivity profile using a vertically pointing cloud radar. Rain rates at the ground are measured directly with disdrometers. All these observations are available with 30 second resolution, but they are also averaged over the grid box appropriate to the various models considered as described below.

Modeled and observed values represent mean values in spatial volumes on very different scales; the range of model grid-box volumes in this study are on the order of 40 – 1000 km³, whereas the 30-second, 60-m measurement volume is approximately 0.0004 km³ assuming a 20 m beamwidth and that, for a 10 m s⁻¹ horizontal wind, 30 s is equivalent to 300 m. For comparison with model grid box values we average the high resolution point observations (Mace *et al.*, 1998; Hogan and Illingworth, 2001) in time and height to match the horizontal and vertical grid spacing of each, although we are aware of the imperfection in this approach (as discussed by Jakob *et al.*, 2004). We use the known horizontal grid box size and model wind speed at each height to calculate the averaging time for the observations in the same manner as Illingworth *et al.* (2007). To make sure that a representative sample of observations is obtained, the

averaging time is limited to a minimum of 10 minutes and a maximum of 1 hour. The resulting averaging time equates to the time taken to advect the air horizontally a distance equivalent to the horizontal size of a model gridbox and assumes that, in the mid-latitudes, the statistics of the observed variability are primarily due to advection over the site rather than *in-situ* evolution and should provide the same statistics as would be obtained from a set of instantaneous spatial observations from around the site (Mace *et al.*, 1998; Hogan and Illingworth, 2001; Illingworth *et al.*, 2007). However, care must be taken when proposing a new model parametrization of a non-linear relationship between precipitation flux and cloud liquid water content that is based on such a comparison (Pincus and Klein, 2000).

A brief description of the precipitation processes in each model is given in section 2. In section 3, the retrieval of observed cloud and precipitation properties by various complementary methods is outlined, and the method of comparing these observations with the corresponding model parameters is then explained. In section 4 we compare the PDF of modeled precipitation fluxes at cloud base and at the ground over eighteen months and compare them with the observed fluxes at both the original 'raw' 30 seconds resolution, and also when averaged over the model grid box. In section 5 we present the statistics of observed liquid water flux and drop size and in section 6 demonstrate that the observed relationship between these two variables is consistent with a physically-based simple scaling analysis based on constant number flux density.

2. Model precipitation schemes

In this paper we compare eighteen months of statistics of the representation of precipitation falling from warm clouds less than 1.5 km deep in four operational models: the European Centre for Medium-Range Weather Forecasts (ECMWF) global model, the Met Office global and mesoscale models, and the Météo France ARPÈGE model. The horizontal and vertical resolutions, together with the forecast lead times, for the versions of the model used in this study, are summarized in Table 1. These models typically hold in each grid box a prognostic cloud liquid water variable, or prognostic water vapour variable from which the condensed cloud liquid water can be diagnosed, which can then be acted on by various source and sink terms relating to condensation and precipitation.

There are three transfer terms within the typical precipitation scheme that involve the warm rain process; autoconversion of liquid water to rain, accretion of liquid water droplets by rain, and evaporation of

TABLE 1: Summary of the four models evaluated in this paper.

Model	Horizontal resolution (km)	Vertical levels	Forecast lead time (hours)
Met Office global	60	38	0–24
Met Office mesoscale	12	38	6–11
ECMWF	40	70	12–35
Météo France ARPÈGE	23	41	12–35

rain. The autoconversion term represents the process by which cloud droplets initially combine through coalescence and collection but is poorly characterised from observations. This term is usually dependent on the model grid-box cloud liquid water content and there may also be a threshold cloud liquid water content, cloud liquid water path or cloud droplet size below which this term is set to zero. The accretion term describes the collection of cloud droplets by falling rain or drizzle drops, while the evaporation of rain or drizzle takes place in the subsaturated air below cloud base. In the Met Office model, the accretion and evaporation rates are determined by the fall speed of the drops and therefore, these rates can be obtained by integrating across an assumed drop size distribution of the rain or drizzle. However, for simplicity and speed, the other two models derive these rates merely in terms of the precipitating liquid water content.

a. Met Office climate and forecasting models

The current large-scale cloud and precipitation scheme in the Met Office Unified Model was described in detail by Wilson and Ballard (1999) and is applicable to both the mesoscale and global versions of the model. In summary, the model holds a prognostic total water content variable (vapour plus liquid) from which cloud fraction and cloud liquid water content are diagnosed using the Smith (1990) scheme. The total water content has a triangular distribution with a width determined by a critical relative humidity value that describes the expected sub-gridscale variability. Various precipitation processes can then act on the total water variable.

For this model the autoconversion term is based on the formulation of Tripoli and Cotton (1980), and the rate of production of rain mixing ratio, q_r , has the form,

$$\frac{dq_r}{dt} = K q_{cl}^{7/3} N_{cl}^{-1/3}, \quad (1)$$

where K is a rate coefficient, q_{cl} is the cloud liquid water mixing ratio, N_{cl} is the the cloud droplet number concentration. Although (1) is in prognostic form, all precipitation produced is assumed to fall to the

surface in one model time step.

The value of N_{cl} is currently a prescribed quantity, $1.5 \times 10^8 \text{ m}^{-3}$ for marine, and $6 \times 10^8 \text{ m}^{-3}$, for continental situations. There is also a critical cloud droplet size, $7 \mu\text{m}$, below which the autoconversion term is set to zero and autoconversion will not deplete liquid water below the corresponding minimum liquid water content (0.9 g m^{-3} over land and 0.2 g m^{-3} over the sea) required to satisfy this critical droplet size.

Raindrops are taken to be spherical with a size distribution given by Marshall and Palmer (1948):

$$n(D) = N_0 \exp(-\Lambda D) = N_0 \exp\left(\frac{-3.67D}{D_0}\right), \quad (2)$$

where $N_0 = 8.0 \times 10^6 \text{ m}^{-4}$, D_0 is the median volume diameter and Λ is the slope of the exponential distribution. Both the accretion rate and the evaporation rate depend on the size and velocity of each falling drop. The accretion term has the form

$$\frac{dq_r}{dt} = \frac{\pi \rho q_{cl}}{4} D^2 v(D), \quad (3)$$

where ρ is the air density and $v(D)$ is the terminal fall speed of the raindrop. The fall speed relationship is expressed as a power law (Sachidananda and Zrnić, 1986), with a correction factor for air density (Pruppacher and Klett, 1978), so that the accretion and evaporation transfer terms are simple to integrate over the raindrop size distribution.

b. ECMWF model

The representation of clouds in the global forecast model of the European Centre for Medium-Range Weather Forecasts (ECMWF) was described in detail by Tiedtke (1993). The model has prognostic cloud fraction and cloud water content, while the ice to liquid ratio is diagnosed from temperature, with diagnostic equations for precipitation. The generation of precipitation is parametrized following Sundqvist (1978):

$$\frac{dq_r}{dt} = K q_{cl} \left(1 - \exp \left[- \left(\frac{q_{cl}}{q_{cl,crit}} \right)^2 \right] \right), \quad (4)$$

where q_{cl} is the cloud liquid water mixing ratio, K is a rate coefficient and there is a critical value $q_{cl,crit}$, set to $3 \times 10^{-4} \text{ kg kg}^{-1}$. Here, rain is again diagnostic and falls to the ground within one timestep. This expression includes both autoconversion and accretion terms in the determination of K and is linear for large q_{cl} . The parameters K and $q_{cl,crit}$ are both set to values based on tuning. There is no explicit size distribution. The evaporation of precipitation is based on the scheme described in Kessler (1969) and only takes place when the gridbox-mean relative humidity is below a threshold value.

c. *Météo France ARPÈGE model*

The representation of clouds in the *Météo France* global forecast model ARPÈGE was described in detail by Ducrocq and Bougeault (1995). The ARPÈGE model cloud and precipitation schemes are fully diagnostic, with cloud fraction diagnosed following Xu and Randall (1996). The generation of precipitation at each level is calculated from the water in excess of the local saturation specific humidity. There are no explicit size distributions or expressions for autoconversion and accretion. The evaporation of precipitation is based on the scheme described in Kessler (1969).

d. *Operational forecasts*

The models are run operationally on a daily, or more frequent, basis, producing forecasts out to at least 36 hours ahead, and hourly profiles (every three hours for the Met Office global model) of model variables over each Cloudnet site were archived as part of the Cloudnet project (Illingworth *et al.*, 2007).

The forecast hours selected from each model are shown in Table 1 and depend on the profiles available and the number of model runs per day. The global versions of the Met Office model and the *Météo France* ARPÈGE are run every 12 hours but only one model run per day is currently selected; the ECMWF global model is run every 24 hours. The Met Office mesoscale model is run every 6 hours and the forecasts between 6 and 11 hours for each of the four runs a day are concatenated to provide a 24 hour segment of model data for each day.

The models hold values of liquid water mixing ratio in each grid box which are converted to liquid water content (LWC) using the model temperature and pressure. Values of liquid water flux (LWF) are held for the lower surface of each grid box in the vertical; it was necessary to run the precipitation scheme offline to obtain these values for the Met Office models. Drop size for the Met Office models is a diagnostic parameter calculated from LWF, but is not available for the other models.

3. Observations

The observations presented in this paper were obtained during Cloudnet (Illingworth *et al.*, 2007), a European project to evaluate the representation of clouds in several operational models using ground-based remote sensing data. In this project, data from the core instruments at each Cloudnet site, a Doppler cloud radar, a lidar, microwave radiometers and a raingauge, are combined into a single dataset on a common grid (Hogan and O’Connor, 2006), with a typical resolution of 30 s and 60 m for the radar and lidar data. This preprocessing greatly assists the subsequent derivation of the microphysical quantities such as liquid water content and liquid water flux.

In this paper, we use observations from the remote sensing site at Chilbolton in southern England (51.1445 N, 358.563 E), which include data from the 94-GHz *Galileo* cloud radar and a Vaisala CT75K lidar ceilometer. We now outline how the microphysical quantities of interest are derived from the observations, and then, the method of comparing the observed quantities with the model values.

a. *Precipitation rates at cloud base*

Cloud base is diagnosed by the sudden increase in lidar backscatter (e.g. Hogan and Illingworth, 2001), and the precipitation rate is estimated from the radar reflectivity using an empirical relationship of the form:

$$\text{LWF} = 9.3 \times 10^{-6} Z^{0.69}, \quad (5)$$

where liquid water flux (LWF) is in $\text{kg m}^{-2} \text{ s}^{-1}$ and radar reflectivity (Z) in $\text{mm}^6 \text{ m}^{-3}$. This relationship is derived from in situ aircraft measurements of drop size spectra (O’Connor *et al.*, 2005).

An accurate method of deriving drizzle liquid water flux and drizzle droplet size below cloud base is possible from combined radar and lidar measurements using the technique described in detail by O’Connor *et al.* (2005), which uses the different scattering properties of liquid drops at the two instrument wavelengths. Because the radar reflectivity is proportional to the sixth power of the diameter and the lidar backscatter signal is approximately proportional to the second power of the diameter, the ratio of the radar to lidar backscatter power is a very sensitive function of mean size (Intrieri *et al.*, 1993). The radar reflectivity also depends on the number concentration of drops within the sample volume and, hence, the higher moments of the drizzle drop distribution, such as drizzle liquid water flux, can be then derived. However, this technique may only be applied in the drizzle below cloud base as the lidar beam is strongly attenuated as soon as it penetrates

the cloud. Comparisons of LWF values below cloud base, where both methods can be applied, show that LWF values obtained from the radar-lidar technique and from radar alone (5) agree to within a factor of two.

We use the accurate radar-lidar technique in section 5, when estimates of drop size are required, but otherwise we use the empirical relationship for this study as it has the advantage that it can be applied both above and below cloud base.

b. Surface rainrate from disdrometer data

A Distromet Joss-Waldvogel Impact Disdrometer RD-69 (Joss and Waldvogel, 1967) installed at Chilbolton provided the drop size distribution of rain reaching the ground presented in this study. The rainrate was then derived by integrating the drop size distribution but is often lower than that measured by conventional raingauges (e.g. Nystuen, 1999). At Chilbolton there are also three rapid response drop-counting rain gauges which count water droplets of known volume as they pass an optical sensor (Norbury and White, 1971; Harden *et al.*, 1978).

The rainrate derived from the disdrometer at Chilbolton has been compared with the rainrates measured by the drop-counting rain gauges for more than one year of continuous data and displays a constant but small underestimate. Therefore, a constant scaling factor of 1.4 has been applied to the disdrometer rainrate used in this paper so that it agrees with the drop-counting rain gauges. Any errors associated with this scaling are assumed to be negligible when looking at a signal that varies by several orders of magnitude. We calculate the median volume diameter from the drops encountered within each 30-s time period to match the temporal resolution of the radar and lidar.

c. Liquid water path

Multi-wavelength microwave radiometers can provide routine measurements of the total column liquid water path, LWP, (Hogg *et al.*, 1983; Westwater, 1993; Crewell *et al.*, 2002). These instruments measure brightness temperatures at two (and sometimes more) microwave frequencies from which the LWP and vapour water path can be retrieved using a suitable microwave absorption model.

The method used in this paper also includes information from a lidar in the retrieval. The lidar is used to check for clear sky periods and the retrieval coefficients are adjusted so that the retrieved LWP is zero during each clear sky period (Gaussiat *et al.*, 2007).

4. The comparison of models and observations

We first present a case study for a single day to illustrate the typical features of observed and modeled light precipitation and highlight some of the major differences between the observed and modeled values. However, we cannot attribute these differences definitively to errors in the model precipitation schemes using only one day of comparisons as this requires that the model forecasts were perfect in all other senses on this particular day. Additional potential sources of error include poor forecasts of the large-scale synoptic fields, such as temperature and humidity, errors in the model cloud schemes that produce the cloud liquid water contents, and retrieval errors in the observations.

A fairer comparison therefore is to evaluate the statistics of the models, where it is assumed that the influence of other sources of error are reduced, and that over eighteen months the statistics of light precipitation in the model may be expected to match the statistics of light precipitation in the observations over the same period.

a. Case study

A continuous deck of stratocumulus cloud was present for the whole day over Chilbolton on 10 October 2003. Figure 1a displays the observed cloud boundaries together with the observed profiles of liquid water flux, and indicates that cloud cover was continuous but that the thickness of cloud varied from 200 m to more than 1 km. In addition, there was a continuous low flux of precipitation from cloud base but generally this evaporated, only reaching the ground from 0430 to 0530 and 1600 to 1700 UTC. The forecast of the vertical profile of LWC and precipitation fluxes over Chilbolton are given in Figs. 1b-e for the four models. All the models have a cloud layer that persisted for much of the day, although the ECMWF layer almost dissipated between 1500 and 2000 UTC and the cloud layer in the Met Office mesoscale model dispersed after 2100 UTC. The values of LWP observed and held in the models are plotted in Fig. 1f, showing that the model LWP is generally within the range of the observations, having values of up to 400 g m^{-2} . As expected, the models do not capture the fine structure of the observed changes with time, and, more importantly, fail to simulate any high LQP values such as those observed between 1600 to 1700 UTC when precipitation reached the surface. This picture is confirmed by Fig. 1g, which compares the liquid water fluxes at the ground. Essentially, all of the precipitation observed at the ground falls in two bursts, one between 1600 and 1700 UTC with a peak 30-second rate of almost 1 mm hr^{-1} , and a second burst between 0430 and 0530 UTC reaching

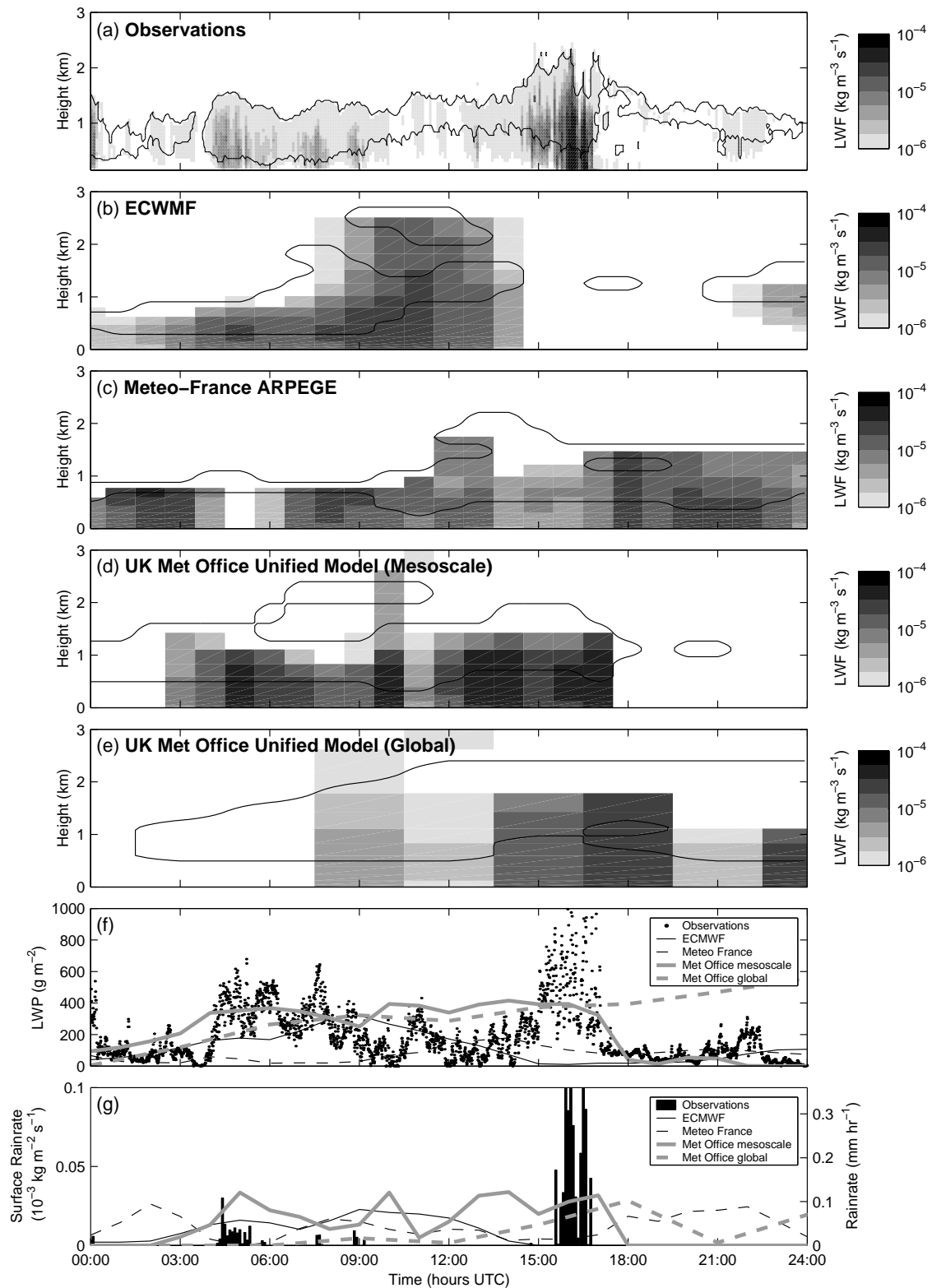


FIG. 1: (a) Observed cloud boundaries (contour lines) and liquid water flux (filled contours in $\text{kg m}^{-3} \text{s}^{-1}$) at Chilbolton, and (b) - (e), the corresponding values for four different operational models for 10 October 2003. Comparisons of (f) the liquid water path (observations in black dots) and (g) the surface rainrate (observations in black bars) for the four forecast models.

0.1 mm hr⁻¹, in contrast to the persistent precipitation rates at the surface of 0.05 mm hr⁻¹ predicted all day by the models. It is instructive to note that all four models, and the observations, have a similar daily mean LWP, and that the mean surface rainrate for the day is also similar. In summary, the details of the temporal changes in LWC and precipitation fluxes vary from model to model, but the general picture is consistent; for a large proportion of the day the models produce light precipitation at cloud base which then falls to the surface with only a small fraction evaporating.

b. Statistics of light precipitation rates over an eighteen month period

The method of extracting suitable profiles is applied to eighteen months of observations and model data. The Cloudnet dataset for this period contains approximately 1,000,000 30-s observed profiles of which a quarter ($\sim 250,000$) satisfy the criteria that there is no precipitation flux at the freezing level and that the warm clouds are < 1.5 km deep. On averaging to the model grid-spacing, this results in 700 to 2500 averaged profiles, depending on the model horizontal grid separation. The corresponding model datasets contain about 13,000 profiles (~ 4300 profiles for the Met Office Global model which outputs every three hours) of which, again, just over a quarter, 4000, match the criteria (1200 for the Met Office Global model.)

These long periods of extensive and persistent low level warm clouds occur about 25% of the time and their presence is generally well captured by the models. Fig. 2 confirms that the PDF of the observed and modelled LWP agree to within 50%. The peak in the observed distribution is close to 0.1 kg m⁻² and the distribution for the global version of the Met Office model is in good agreement. The shape of the PDF for the other models has the same form as the observations but they tend to underestimate LWP when greater than 0.3 kg m⁻². The peak of the distribution for the mesoscale version of the Met Office model is shifted below that of the other models. We conclude that any large overestimate of precipitation rate at cloud base in any model is unlikely to be attributable to an overestimate of the amount of liquid water.

Figure 3 shows the probability density of the observed LWF at cloud base (from radar-lidar method O'Connor *et al.*, 2005), and at the ground (from disdrometer). The change in the shape of the PDFs is immediately obvious; the frequency of LWF $< 10^{-5}$ kg m⁻² s⁻¹ is dramatically reduced at the ground, compared to cloud base, whereas for higher fluxes there is a much smaller change in frequency.

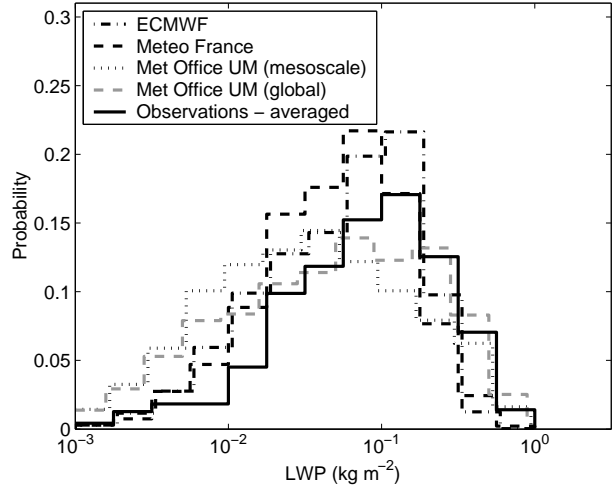


FIG. 2: Probability density functions of observed and modeled liquid water path at Chilbolton for the 18 months April 2003 to September 2004. The observed PDF was derived from observations averaged to the ECMWF model grid-spacing. The individual PDFs have been offset slightly with respect to each other to improve clarity.

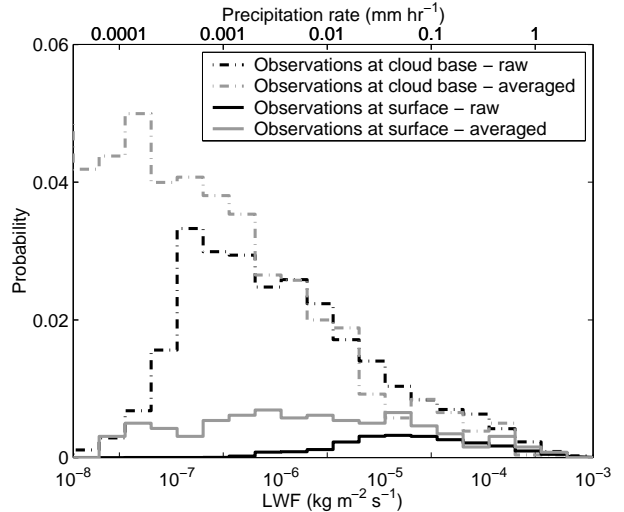


FIG. 3: Probability density function of observed liquid water flux at cloud base over Chilbolton for the 18 months April 2003 to September 2004. The PDFs were calculated for observations at the original raw 30-s resolution and for observations averaged to the ECMWF model grid-spacing.

The reduction in frequency is a signature of evaporation and, if we assume that LWF is a function of drop size and not drop number, then this change in the shape of the PDFs, which is most striking for the raw observations, can be attributed to the preferential evaporation of the smaller drops as they fall to the surface.

The sharp drop-off in the raw LWF values below 10^{-7} kg m⁻² s⁻¹, or $Z = -28$ dBZ, is attributable to the limited radar sensitivity. The effect of averaging

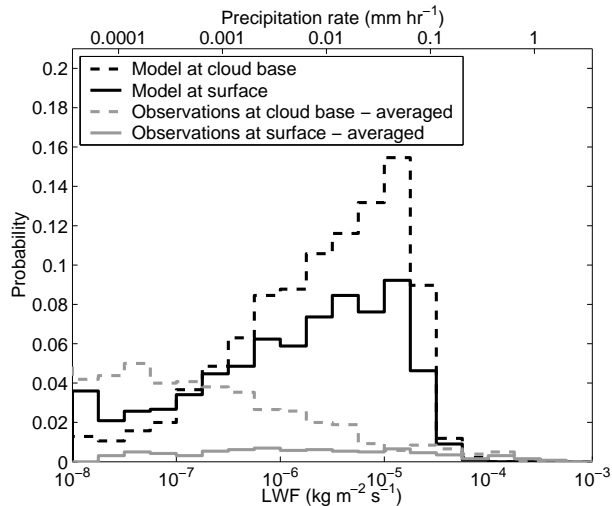


FIG. 4: Probability density functions of observed and ECMWF model liquid water flux at cloud base and at the surface at Chilbolton for the 18 months April 2003 to September 2004. The observed PDF was derived from observations averaged to the ECMWF model grid-spacing.

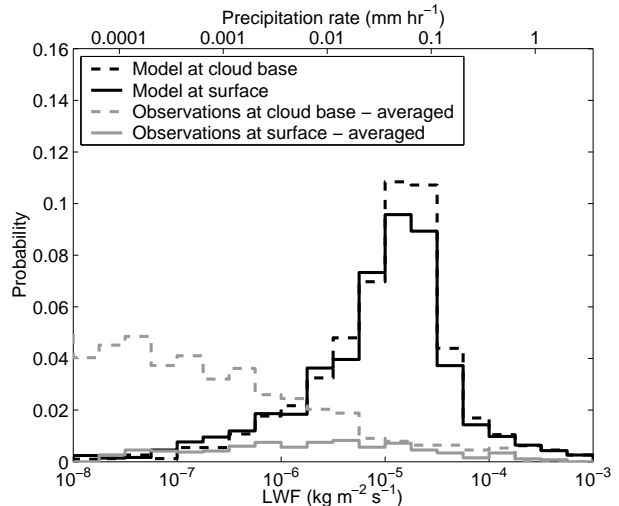


FIG. 5: Same as Fig. 4 except for the Météo France model with the observed PDF averaged to the Météo France model grid-spacing.

the LWF to a model grid (the ECMWF model grid spacing has been chosen here) tends to shift LWF towards lower values. About 24% of the individual raw profiles contain LWF $> 10^{-7} \text{ kg m}^{-2} \text{ s}^{-1}$ at cloud base, whereas at the surface the number of raw profiles above this threshold falls to less than 3%. After averaging to the model grid-spacing 24% of the observed profiles contain LWF $> 10^{-7} \text{ kg m}^{-2} \text{ s}^{-1}$ at cloud base but the number of averaged profiles above this threshold at the surface is now 7%.

The mean surface precipitation rates for both Met Office models ($4.5 \times 10^{-5} \text{ kg m}^{-2} \text{ s}^{-1}$) and Météo France ($2.5 \times 10^{-5} \text{ kg m}^{-2} \text{ s}^{-1}$) agree with the observed precipitation rate ($3.5 \times 10^{-5} \text{ kg m}^{-2} \text{ s}^{-1}$, $2.5 \times 10^{-5} \text{ kg m}^{-2} \text{ s}^{-1}$ when averaged to a 3-hourly timestep) to within a factor of two, which is comparable with the expected error in the rainrate measurements. The ECMWF model, however, has a mean surface precipitation rate almost an order of magnitude lower than observed, at $5 \times 10^{-6} \text{ kg m}^{-2} \text{ s}^{-1}$.

The probability density of precipitation rates at cloud base and at the surface are presented in Figs. 4-7 for each model and for observations averaged to the appropriate model grid-spacing. The first point to note is that all models overpredict the frequency of LWF between 10^{-6} and $10^{-4} \text{ kg m}^{-2} \text{ s}^{-1}$ (approximately $0.003 - 0.3 \text{ mm hr}^{-1}$) at both cloud base and at the surface, even for those models where the mean precipitation rate at the surface is in agreement. The second is that the PDF of precipitation rate at the surface is very different to what is observed.

The ECMWF model (Fig. 4) produces precipita-

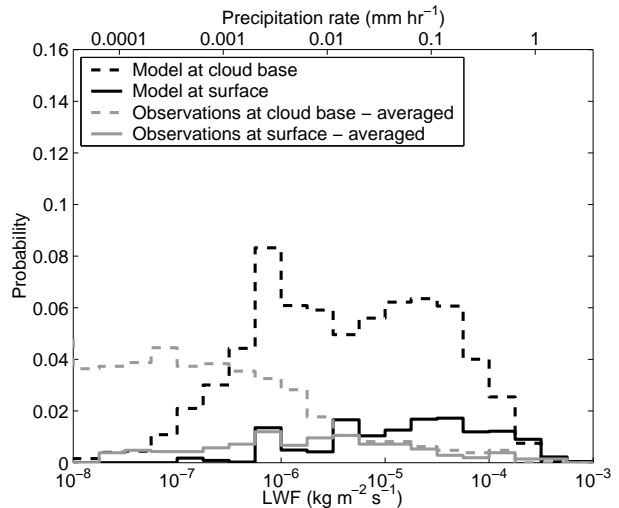


FIG. 6: Same as Fig. 4 except for the Met Office Mesoscale model with the observed PDF averaged to the Met Office Mesoscale model grid-spacing.

tion rates less than 0.1 mm hr^{-1} at cloud base much more frequently than is observed, and the frequency at the surface of this range of precipitation rates is reduced by much less than 50%. The observations have a quite different character and reveal that for precipitation rates down to 0.01 and 0.001 mm hr^{-1} the evaporation is very high, as would be expected for the smaller droplets in these very low precipitation rates. The Météo France model (Fig. 5) shows a similar behavior, in that precipitation rates less than 0.1 mm hr^{-1} at cloud base are too frequent, and there is insufficient evaporation as the drops fall to the surface. These difficulties with the evaporation are prob-

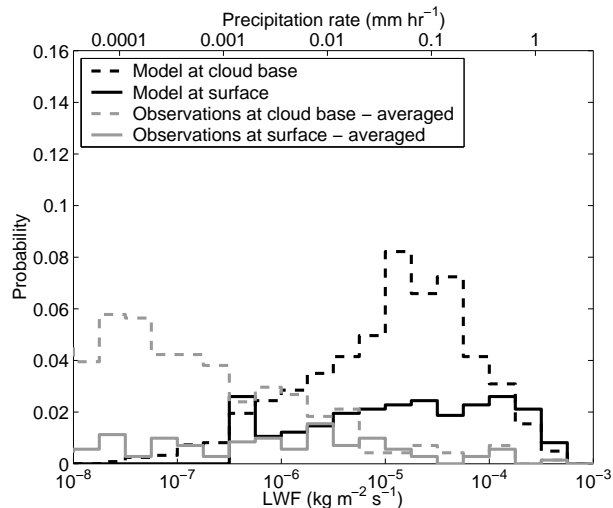


FIG. 7: Same as Fig. 4 except for the Met Office Global model with the observed PDF averaged to the Met Office Global model grid-spacing.

ably associated with the lack of an implicit change in drop size with precipitation rate in the ECMWF and Météo France models. In contrast to this the two Met Office models (Figs. 6 and 7) still produce precipitation rates less than 0.1 mm hr^{-1} too frequently but there is much more evaporation, and the proportion which evaporates increases as the precipitation rate becomes less. The improved performance of the Met Office model, especially for lower precipitation rates, is consistent with the use of an explicit drop spectrum in the model; very low precipitation rates are associated with smaller sized droplets which evaporate more rapidly. Although the performance of the Met Office model is an improvement, Figs. 6 and 7 demonstrate that for precipitation rates above 0.03 mm hr^{-1} , the evaporation rate is still too low. If the terminal velocity is proportional to the size of the droplets, then it is easy to show that, for a given subsaturation, the survival distance of the drops varies as the cube of the droplet diameter. In Section 5 we suggest that assumed Marshall-Palmer size spectrum in the Met Office model implies drop sizes much larger than those actually observed for these light precipitation rates.

c. Humidity profiles

For a given drop size the survival time below cloud base is proportional to the subsaturation, so it is possible that the model relative humidity is much too high and that this is responsible for the underestimate of the amount of evaporation. To examine this we compare the median relative humidity below cloud base from each of the four models with the observed median relative humidity below cloud base

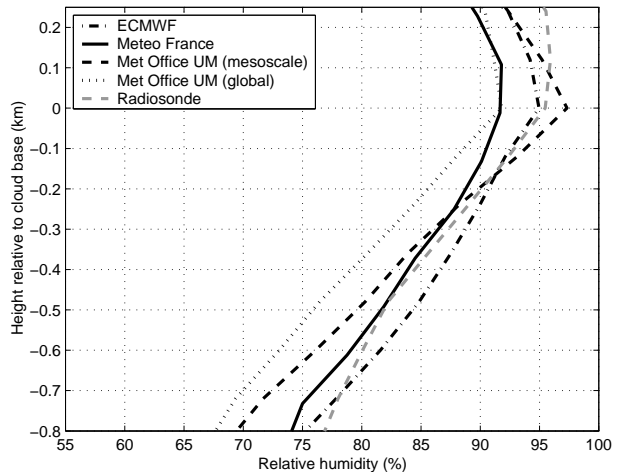


FIG. 8: Median observed and modeled relative humidity below cloud base at Chilbolton for the 18 months April 2003 to September 2004.

derived from radiosondes released at Larkhill 25 km away from Chilbolton. Figure 8 shows that model grid-boxes only partially filled with cloud (i.e. cloud fraction less than one) often have relative humidity values less than 100% at nominal cloud base. The same is true of radiosonde ascents, which, as a point measurement, would not always be expected to pass through a cloud. Figure 8 indicates that any biases in the models are generally less than 5% and cannot explain the large discrepancy in the modeled and observed evaporation rates.

5. Statistics of drizzle drop size spectra

We now present the observed statistics of liquid water flux versus drizzle drop size at the raw 30-s resolution. The statistics in Fig. 3 suggest that drizzle rates generally decrease rapidly below cloud base due to evaporation, so that even appreciable drizzle at cloud base may not reach the surface (Bretherton *et al.*, 2004; Wood, 2005). Figures 4 -7 indicate that this is not captured adequately in models. We now explore the validity of assuming that drizzle follows a typical rain size distribution such as that given by Marshall and Palmer (1948) as used by the Met Office and by Chen and Cotton (1987).

The Met Office Unified Model precipitation scheme describes LWF in terms of an explicit size distribution, which allows a direct comparison with observations if we assume that the observed drizzle drop size distribution can be represented by an exponential distribution similar to that in (2). In Fig. 9 the relationship between the observed values of the median volume diameter, D_0 , and the observed LWF is shown together with the same relationship for the model. LWF in the model is calculated using the

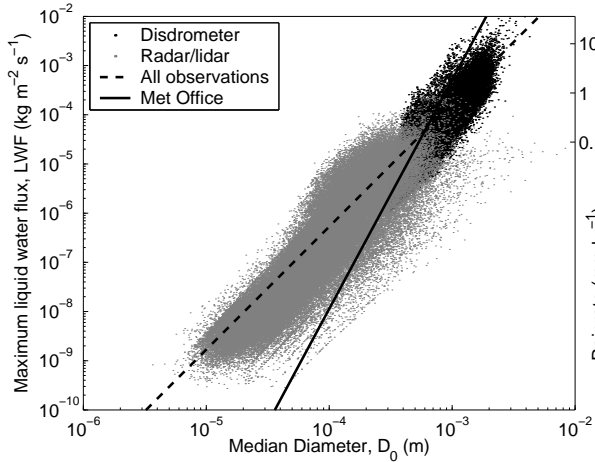


FIG. 9: Scatter plot of the observations (points) at the raw 30-s resolution and Met Office mesoscale model values (solid line) for median volume diameter versus maximum liquid water flux for the 12 months April 2003 to March 2004. Disdrometer observations are shown in black and include all rain recorded in the period, radar/lidar observations in grey. Superimposed is the least-squares fit using linear piecewise-means to the observations (dashed).

size distribution given in (2) so that, although there is some slight variation in fall speed due to air density, all points fall on the same line. The observed values of D_0 below about 0.5 mm are derived from radar and lidar data, while larger sizes are measured by the disdrometer. Note that observed values of D_0 derived from radar and lidar data are only available below cloud base.

The observed values derived from both disdrometer and radar-lidar show consistency and have the same relative spread for a given value of LWF; a consequence of the variability in the drizzle droplet number concentration. The least-squares fit to the piecewise-means of the observations is significantly different to the model relationship and illustrates that the model precipitation scheme is clearly overestimating the drop size for $D_0 < 0.5$ mm.

Previous findings have relaxed the assumption of a constant N_0 in model relationships. The formula given by Thompson *et al.* (2004) utilised lower- and upper-intercept limits with a gradual transition from one to the other across the range of sizes corresponding to drizzle. This was chosen to simulate the lower terminal fall velocities of drizzle before returning to a Marshall-Palmer value for the upper-intercept limit at larger sizes. The effect of averaging the observed spectra to model grids, however, is uncertain and any parametrization must take into account the issue of sub-grid-scale variability.

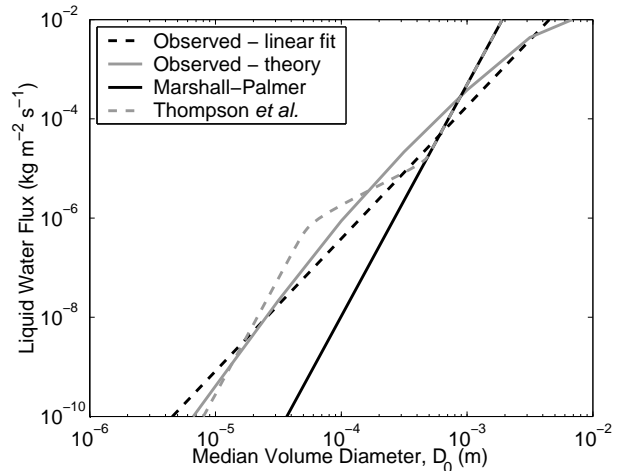


FIG. 10: Least-squares fit using linear piecewise-means to the 30-s observations in Fig. 9 (denoted 'Observed - linear fit'), the relationship derived from a simple scaling analysis ('Theory') assuming number flux density is constant as described in section 6, and two model relationships (see text).

6. Investigating the relationship between drizzle rate and drizzle drop size

The Met Office scheme assumes that both rain and drizzle size distributions have the same constant value of the N_0 parameter in (2) leading to the solid line in Fig. 9 and a relationship between LWF and D_0 of the form

$$\text{LWF} = 5.52 \times 10^{10} D_0^{4.67}. \quad (6)$$

However, the best fit to the observed data points is

$$\text{LWF} = 5.37 \times 10^3 D_0^{2.50}. \quad (7)$$

This suggests that the assumption of constant N_0 is not appropriate for drizzle. In this section we derive a more appropriate relationship for drizzle and explain it physically.

a. The variation of the intercept parameter with the median volume diameter

An adjustment of the model LWF calculation so that it agrees with the fit to the observations in Fig. 9 can be achieved in a simple manner by making the N_0 parameter vary as function of D_0 . To do this we first define LWF as

$$\text{LWF} = \frac{\rho_l \pi}{6} \int_0^\infty n(D) D^3 v(D) dD, \quad (8)$$

where ρ_l is the density of liquid water, $n(D) dD$ is the number concentration of water droplets with diameters between D and $D+dD$ and $v(D)$ is the terminal velocity of individual water drops. It is assumed that

$n(D)$ is represented by (2), except with N_0 is a function of D_0 , and that $v(D)$ follows a power law

$$v(D) = eD^f, \quad (9)$$

where e is a constant and f may vary from 0.5 for large drops to 2 for small droplets in the Stokes regime. An appropriate value for drizzle drops in the range $80 \mu\text{m} < D < 1 \text{ mm}$ is $f = 1$ (e.g. Rogers and Yau, 1989); the Met Office scheme uses $f = 0.67$, more suitable for larger raindrops. Integration of (8) over all drop sizes with N_0 constant gives

$$\text{LWF} = \frac{\rho_l \pi e \Gamma(4+f)}{6 \cdot 3.67^{4+f}} N_0 D_0^{4+f}, \quad (10)$$

where Γ denotes the gamma function and the factor 3.67 arises from the exponent in (2).

Assuming a power law relationship $N_0 \propto D_0^k$, integration of (8) gives

$$\text{LWF} = aD_0^{(4+f+k)} = aD_0^{2.50}, \quad (11)$$

where a is the prefactor in (7) and leads to

$$N_0 = cD_0^{-(1.5+f)}, \quad (12)$$

where the prefactor c varies slightly with the choice of f . If $f = 1$, reasonable for drizzle drops, then $c = 0.73$, whereas if $f = 0.67$, as in the Met Office scheme, then $c = 0.77$.

b. Explaining the intercept parameter variations in terms of number flux density

The result given in (12) indicates that there is some moment of the distribution which remains constant. Once drops reach a diameter of $60 \mu\text{m}$ the dominant mode of growth is by collision and coalescence (e.g. Rogers and Yau, 1989). If we assume a steady-state profile of LWF then we might expect the number of drizzle drops, once generated, to remain constant over the time it takes a drop to fall. As the drops fall they increase in size through collision and coalescence but are also falling faster. If the falling drops do not collide with other falling drops, only cloud droplets, then the number flux density is constant. With this assumption we can write

$$\int n(D)v(D)dD = c, \quad (13)$$

where the constant c is fixed, and we can then integrate over all drop sizes in the same manner as (10);

$$\frac{e \Gamma(1+f)}{3.67^{(1+f)}} N_0 D_0^{(1+f)} = c \quad (14)$$

and obtain the result

$$N_0 \propto D_0^{-(1+f)}. \quad (15)$$

This is in reasonable agreement with the observations (11) and the deviation of the observed exponent by 0.5 from the theoretical value indicates that the observed number flux density decreases as the drops grow. This suggests that the number concentration of drizzle drops is high enough that capture of smaller falling drops by larger ones occurs in significant numbers. The full expression given by Beard (1976) can be used to represent $v(D)$, which is also displayed in Fig. 10 as the line 'Theory'. This line and the linear fit are not significantly different over the range of relevant drop sizes.

A similar analysis (and suggested improvement) cannot be performed for the ECMWF and Météo France models since they do not describe the liquid water flux in terms of an explicit size distribution.

7. Conclusion

An analysis has been carried out of precipitation rates at cloud base and at the surface over a period of 18 months for occasions when there was no precipitation flux at the freezing level but warm clouds less than 1.5 km deep were present. Precipitation rates at cloud base and the surface were observed every 30 seconds and then compared with the precipitation rates held in four operational forecasting models. Over one million observations and 4,000 hours of model data fulfilled the criterion. The PDF of the modelled and observed values of liquid water path were similar, as were the cloud bases and tops, indicating that model liquid water contents were reasonably accurate. However, the models produced light precipitation rates, $< 0.1 \text{ mm hr}^{-1}$, at cloud base much more frequently than was observed, and, in addition, these light precipitation rates survived the journey to the ground far more frequently than observed. The average precipitation rates for the model and observations were in general agreement, but this was because the observations showed occasional bursts of heavier rain which were not simulated by the models. The underestimate of the sub-cloud evaporation was most marked with the ECMWF and Météo France models, especially at the lighter precipitation rates, and we suggest that this is because the evaporation schemes in these models have no implied drop size spectra. The Met Office model was able to capture the evaporation of the very light precipitation rates below 0.03 mm hr^{-1} and we believe this is because it has an implicit Marshall-Palmer drop size distribution so that these very low precipitation rates had very small drops which could evaporate more quickly. However, for precipitation rates in the range 0.03 to 1 mm hr^{-1} the evaporation in the Met Office model was still too low and this may be because the assumed Marshall-Palmer drop size spectrum leads to drops which are

larger than those observed. We propose that at these low precipitation rates it would be more appropriate to have a drop spectrum with a larger concentration and smaller drops than currently assumed.

Acknowledgements

We acknowledge the Cloudnet project (European Union contract EVK2-2000-00611) for providing the drizzle and liquid water path dataset, the Met Office mesoscale and global model data, the ECMWF model data and the Météo France model data, which was produced by the University of Reading, Met Office, ECMWF and Météo France. This research was funded by Met Office grant PB/B4301 and NERC contract NE/D005205/1. We appreciate Anthony Del Genio's helpful comments and the comments of the anonymous referees.

REFERENCES

- Albrecht, B. A., Bretherton, C. S., Johnson, D., Schubert, W. H., and Frisch, A. S., 1995: The Atlantic Stratocumulus Transition Experiment — ASTEX. *Bull. Amer. Meteorol. Soc.*, **76**(6), 889–904.
- Beard, K. V., 1976: Terminal velocity and shape of cloud and precipitation drops aloft. *J. Atmos. Sci.*, **33**, 851–864.
- Bretherton, C. S., Uttal, T., Fairall, C. W., Yuter, S. E., Weller, R. A., Baumgardner, D., Comstock, K., Wood, R., and Raga, G. B., 2004: The Epic 2001 stratocumulus study. *Bull. Amer. Meteorol. Soc.*, **85**(7), 967–977.
- Caldwell, P., Bretherton, C. S., and Wood, R., 2005: Mixed-layer budget analysis of the diurnal cycle of entrainment in Southeast Pacific stratocumulus. *J. Atmos. Sci.*, **62**(10), 3775–3791.
- Chen, C. and Cotton, W. R., 1987: The physics of the marine stratocumulus-capped mixed layer. *J. Atmos. Sci.*, **44**(20), 2951–2977.
- Comstock, K. K., Wood, R., Yuter, S. E., and Bretherton, C. S., 2004: Reflectivity and rain rate in and below drizzling stratocumulus. *Q. J. R. Meteorol. Soc.*, **130**, 2891–2918.
- Crewell, S., Drusch, M., Van Meijgaard, E., and Lammeren, A. V., 2002: Cloud Observations and Modelling within the European BALTEX Cloud Liquid Water Network. *Boreal Environment Research*, **7**, 235–245.
- Driedonks, A. G. M. and Duynkerke, P. G., 1989: Current problems in the stratocumulus-topped ABL. *Boundary-Layer Meteorol.*, **46**, 275–303.
- Ducrocq, V. and Bougeault, P., 1995: Simulations of an observed squall line with a meso-beta scale hydrostatic model. *Wea. Forecasting*, **10**, 380–399.
- Feingold, G., Stevens, B., Cotton, W. R., and Frisch, A. S., 1996: The relationship between drop in-cloud residence time and drizzle production in numerically simulated stratocumulus clouds. *J. Atmos. Sci.*, **53**(8), 1108–1122.
- Feingold, G., Boers, R., Stevens, B., and Cotton, W. R., 1997: A modeling study of the effect of drizzle on cloud optical depth and susceptibility. *J. Geophys. Res. — Atmos.*, **102**(D12), 13527–13534.
- Fox, N. I. and Illingworth, A. J., 1997: The retrieval of stratocumulus properties by ground based radar. *J. Appl. Meteorol.*, **36**, 485–492.
- Gaussiat, N., Hogan, R. J., and Illingworth, A. J., 2007: Accurate liquid water path retrieval from low-cost microwave radiometers using additional information from lidar and operational forecast models. *J. Atmos. Ocean. Technol.*, **24**, 1562–1575.
- Harden, B. N., Norbury, J. R., and White, W. J. K., 1978: Attenuation/rain-rate relationships on terrestrial microwave links in the frequency range 10–40 GHz. *Electron. Lett.*, **14**, 154–155.
- Harrison, E. F., Minnis, P., Barkstrom, B. R., Ramanathan, V., Cess, R. D., and Gibson, G. G., 1990: Seasonal variation of cloud radiative forcing derived from the Earth Radiation Budget Experiment. *J. Geophys. Res.*, **95**, 18687–18704.
- Hartmann, D. L., Ockert-Bell, M. E., and Michelsen, M. L., 1992: The effect of cloud type on earth’s energy balance: Global analysis. *J. Climate*, **5**(11), 1281–1304.
- Hogan, R. J., C. J. and Illingworth, A. J., 2001: Comparison of ECMWF winter-season cloud fraction with radar-derived values. *J. Appl. Meteorol.*, **40**, 513–525.
- Hogan, R. J. and O’Connor, E. J., 2006: *Facilitating cloud radar and lidar algorithms: the Cloudnet Instrument Synergy/Target Categorization product*. Cloudnet documentation: <http://www.cloudnet.org/data/products/categorize.html>.
- Hogg, D. C., Guiraud, F. O., Snider, J. B., Decker, M. T., and Westwater, E. R., 1983: A steerable dual-channel microwave radiometer for measurement of water vapor and liquid in the troposphere. *J. Appl. Meteorol.*, **22**(5), 789–806.
- Hudson, J. G. and Yum, S. S., 2001: Maritime-continental drizzle contrasts in small cumuli. *J. Atmos. Sci.*, **58**, 915–926.
- Illingworth, A. J., Hogan, R. J., O’Connor, E. J., Bouniol, D., Brooks, M. E., Delanoë, J., Donovan, D. P., Eastment, J. D., Gaussiat, N., Goddard, J. W. F., Haeffelin, M., Baltink, H. K., Krasnov, O., Pelon, J., Piriou, J.-M., Protat, A., Russchenberg, H., Seifert, A., Tompkins, A. M., van Zadelhoff, G.-J., Vinit, F., Willén, U., Wilson, D. R., and Wrench, C. L., 2007: CLOUDNET - continuous evaluation of cloud profiles in seven operational models using ground-based observations. *Bull. Amer. Meteorol. Soc.*, **88**, 883–898.
- Intrieri, J. M., Stephens, G. L., Eberhard, W. L., and Uttal, T., 1993: A method for determining cirrus cloud particle sizes using lidar and radar backscatter technique. *J. Appl. Meteorol.*, **32**, 1074–1082.

- Jakob, C., 1999: Cloud cover in the ECMWF reanalysis. *J. Climate*, **12**(4), 947–959.
- Jakob, C., 2003: An improved strategy for the evaluation of cloud parameterizations in GCMs. *Bull. Amer. Meteorol. Soc.*, **84**(10), 1387–1401.
- Jakob, C., Pincus, R., Hannay, C., and Xu, K.-M., 2004: Use of cloud radar observations for model evaluation: A probabilistic approach. *J. Geophys. Res. — Atmos.*, **109**, doi:10.1029/2003JD003473.
- Joss, J. and Waldvogel, A., 1967: Ein spektrograph fuer niederschlagstropfen mit automatischer auswertung. *Pure Appl. Geophys.*, **68**, 240–246.
- Kessler, E., 1969: On the distribution and continuity of water substance in atmospheric circulation. In *Meteorological Monographs*, volume 10, page 84. Americ. Meteor. Soc., Boston, MA.
- Mace, G. G., Jakob, C., and Moran, K. P., 1998: Validation of hydrometeor occurrence predicted by the ecmwf model using millimeter wave radar data. *Geophys. Res. Lett.*, **25**(10), 1645–1648.
- Marshall, J. S. and Palmer, W. M., 1948: The distribution of raindrops with size. *J. Atmos. Sci.*, **5**(4), 165–166.
- Nicholls, S., 1984: The dynamics of stratocumulus: Aircraft observations and comparisons with a mixed layer model. *Q. J. R. Meteorol. Soc.*, **110**, 783–820.
- Norbury, J. R. and White, W. J., 1971: A rapid-response rain gauge. *Journal of Physics E: Scientific Instruments*, **4**, 601–602.
- Nystuen, J. A., 1999: Relative performance of automatic rain gauges under different rainfall conditions. *J. Atmos. Ocean. Technol.*, **16**, 1025–1043.
- O’Connor, E. J., 2003: *Radar and lidar studies of Stratocumulus*. Ph.D. thesis, University of Reading, UK.
- O’Connor, E. J., Hogan, R. J., and Illingworth, A. J., 2005: Retrieving stratocumulus drizzle parameters using doppler radar and lidar. *J. Appl. Meteorol.*, **44**(1), 14–27.
- Paluch, I. R. and Lenschow, D. H., 1991: Stratiform cloud formation in the marine boundary layer. *J. Atmos. Sci.*, **48**(19), 2141–2158.
- Pincus, R. and Klein, S. A., 2000: Unresolved spatial variability and microphysical process rates in large-scale models. *J. Geophys. Res.*, **105**, doi:10.1029/2000JD900504.
- Pruppacher, H. R. and Klett, J. D., 1978: *Microphysics of clouds and precipitation*. D. Reidel Publishing Company, Boston.
- Ramanathan, V., Cess, R. D., Harrison, E. F., Minnis, P., Barkstrom, B. R., Ahmad, E., and Hartmann, D., 1989: Cloud-radiative forcing and climate: Results from the Earth Radiation Budget Experiment. *Science*, **243**, 57–63.
- Rogers, R. R. and Yau, M. K., 1989: *A short course in cloud physics*. Oxford : Pergamon, 3rd edition.
- Sachidananda, M. and Zrnić, D. S., 1986: Differential propagation phase shift and rainfall rate estimation. *Radio Sci.*, **21**, 235–247.
- Smith, R. N. B., 1990: A scheme for predicting layer clouds and their water content in a general circulation model. *Q. J. R. Meteorol. Soc.*, **116**, 435–460.
- Stephens, G. L., Vane, D. G., Boain, R. J., Mace, G. G., Sassen, K., Wang, Z., Illingworth, A. J., O’Connor, E. J., Rossow, W. B., Durden, S. L., Miller, S. D., Austin, R. T., Benedetti, A., Mitrescu, C., and the CloudSat Science Team, 2002: The CloudSat mission and the A-train. *Bull. Amer. Meteorol. Soc.*, **83**(12), 1771–1790.
- Sundqvist, H., 1978: A parameterization scheme for non-convective condensation including prediction of cloud water content. *Q. J. R. Meteorol. Soc.*, **104**, 677–690.
- Thompson, G., Rasmussen, R. M., and Manning, K., 2004: Explicit forecasts of winter precipitation using an improved bulk microphysics scheme. Part I: description and sensitivity analysis. *Mon. Weather Rev.*, **132**(2), 519–542.
- Tiedtke, M., 1993: Representation of clouds in large-scale models. *Mon. Weather Rev.*, **121**, 3040–3061.
- Tripoli, G. J. and Cotton, W. R., 1980: A numerical investigation of several factors contributing to the observed variable intensity of deep convection over south Florida. *J. Appl. Meteorol.*, **19**, 1037–1063.
- van Zanten, M. C., Stevens, B., Vali, G., and Lenschow, D. H., 2005: Observations of drizzle in nocturnal marine stratocumulus. *J. Atmos. Sci.*, **62**(1), 88–106.
- Webb, M., Senior, C., Bony, S., and Morcrette, J.-J., 2001: Combining ERBE and ISCCP data to assess clouds in the Hadley Centre, ECMWF and LMD atmospheric climate models. *Climate Dynamics*, **17**(12), 905–922.

- Westwater, E. R., 1993: Ground-based microwave remote sensing of meteorological variables. In M. A. Janssen, editor, *Atmospheric remote sensing by microwave radiometry*, pages 145–213. John Wiley & Sons, New York.
- Wilson, D. R. and Ballard, S. P., 1999: A microphysically based precipitation scheme from the UK Meteorological Office Unified Model. *Q. J. R. Meteorol. Soc.*, **125**, 1607–1636.
- Wood, R., 2005: Drizzle in stratiform boundary layer clouds. Part I: vertical and horizontal structure. *J. Atmos. Sci.*, **62**(9), 3011–3033.
- Wood, R. and Bretherton, C. S., 2004: Boundary layer depth, entrainment, and decoupling in the cloud-capped subtropical and tropical marine boundary layer. *J. Climate*, **17**(18), 3576–3588.
- Xu, K.-M. and Randall, D. A., 1996: A semiempirical cloudiness parameterization for use in climate models. *J. Atmos. Sci.*, **53**(21), 3084–3102.